Systematic and Applied Microbiology 42 (2019) 506–516

Contents lists available at ScienceDirect

Systematic and Applied Microbiology

journal homepage: http://www.elsevier.com/locate/syapm

Cutibacterium avidum is phylogenetically diverse with a subpopulation being adapted to the infant gut

Vanesa Natalin Rocha Martin[a,b], Christophe Lacroix[a], Jiri Killer[c], Vera Bunesova[d], Evelyn Voney[a], Christian Braegger[b], Clarissa Schwab[a,*]

[a] Laboratory of Food Biotechnology, Institute of Food, Nutrition and Health, ETH-Zurich, 8092 Zurich, Switzerland
[b] Division of Gastroenterology and Nutrition, University Children's Hospital Zurich, 8032 Zurich, Switzerland
[c] Institute of Animal Physiology and Genetics, Academy of Sciences of the Czech Republic, Czech Republic
[d] Department of Microbiology, Nutrition and Dietetics, Czech University of Life Sciences Prague, Kamýcká 129, Prague 6, Suchdol 165 00, Czech Republic

ARTICLE INFO

Article history:
Received 1 March 2019
Received in revised form 9 May 2019
Accepted 10 May 2019

Keywords:
Cutibacterium avidum
Infant gut microbiota
Bifidobacterium
Cross-feeding
Glucuronic acid

ABSTRACT

The infant gut harbors a diverse microbial community consisting of several taxa whose persistence depends on adaptation to the ecosystem. In healthy breast-fed infants, the gut microbiota is dominated by *Bifidobacterium* spp.. *Cutibacterium avidum* is among the initial colonizers, however, the phylogenetic relationship of infant fecal isolates to isolates from other body sites, and *C. avidum* carbon utilization related to the infant gut ecosystem have been little investigated.

In this study, we investigated the phylogenetic and phenotypic diversity of 28 *C. avidum* strains, including 16 strains isolated from feces of healthy infants. We investigated the *in vitro* capacity of *C. avidum* infant isolates to degrade and consume carbon sources present in the infant gut, and metabolic interactions of *C. avidum* with infant associated *Bifidobacterium longum* subsp. *infantis* and *Bifidobacterium bifidum*.

Isolates of *C. avidum* showed genetic heterogeneity. *C. avidum* consumed D- and L-lactate, glycerol, glucose, galactose, N-acetyl-D-glucosamine and maltodextrins. Alpha-galactosidase- and β-glucuronidase activity were a trait of a group of non-hemolytic strains, which were mostly isolated from infant feces. Beta-glucuronidase activity correlated with the ability to ferment glucuronic acid. Co-cultivation with *B. infantis* and *B. bifidum* enhanced *C. avidum* growth and production of propionate, confirming metabolic cross-feeding.

This study highlights the phylogenetic and functional diversity of *C. avidum*, their role as secondary glycan degraders and propionate producers, and suggests adaptation of a subpopulation to the infant gut.

Introduction

Cutibacterium spp. are gram-positive, non-spore forming, anaerobic-to-aerotolerant bacteria that belong to the phylum Actinobacteria. *Cutibacterium* were formerly classified as *Propionibacterium* and are able to ferment lactate and monosaccharides (e.g. glucose, galactose) to propionate, acetate and CO_2 [45,58,72]. The genus *Cutibacterium* includes the species *Cutibacterium acnes, Cutibacterium granulosum* and *Cutibacterium avidum. C. acnes* and *C. granulosum* colonize oily surfaces of the skin, while *C. avidum* is adapted to wet regions like the axilla, groin and rectum [39]. The pathogenic potential of the different species is under discussion [11,35]. Hemolytic activity has been observed for *C. acnes* and *C. avidum* but does not seem related to virulence [34,55]. *C. avidum* has been sporadically associated with breast and post-surgery infections [11], but also to healthy breast tissue [66]. *C. avidum* has been frequently isolated from infant feces [24,29,50], and was recently suggested as a common infant gut colonizer and contributor to intestinal propionate formation in infants under 3 months of age. Isolates of *C. avidum* from infant feces were shown to colonize a continuous *in vitro* fermentation model mimicking the conditions in the proximal colon, indicating adaptation to the infant gastrointestinal tract [55]. *In vivo C. avidum* persistence depended on initial colonization levels as well as on microbe-microbe interactions, especially with lactate producers such as *Bifidobacterium* [55].

In healthy infants, *Bifidobacterium* spp. are among the major genera in the gut during the first year of life [5,62]. *Bifidobacterium longum* subsp. *infantis* and *Bifidobacterium bifidum* are two

* Corresponding author.
E-mail address: clarissa.schwab@hest.ethz.ch (C. Schwab).

https://doi.org/10.1016/j.syapm.2019.05.001
0723-2020/

Table 1
List of *C. avidum* strains used in this study.

Strain ID	Source	Donor	Age of donor (months)	Isolation medium	RFLP pattern	Hemolysis	References
C. avidum ATCC 25577	Oral cavity	–[a]	–	–	–	Positive[b]	[22]
C. avidum P4118	Infant feces	–	0.5	Postgate E	3	Negative	[50]
C. avidum P336	Infant feces	N1	1	Beerens agar	5	Positive	[24]
C. avidum P337	Infant feces	N4	1	Wilkens-Chalgren agar	1	Positive	[24]
C. avidum P279	Infant feces	6	3	YEL + M + K[c]	4	Negative	[55]
C. avidum P280	Infant feces	7	1.5	YEL + M + K	2	Negative	[55]
C. avidum P316	Infant feces	7	1.5	YEL + M + K	1	Positive	[55]
C. avidum P315	Infant feces	1	1.5	YEL + M + K	1	Positive	[55]
C. avidum P277	Infant feces	1	1.5	YEL + M+ K	2	Negative	[55]
C. avidum P338	Infant feces	11	0.5	YEL + M + K	5	Negative	[55]
C. avidum P339	Infant feces	11	0.5	YEL + M + K	2	Negative	[55]
C. avidum P311	Infant feces	2	2	YEL + M + K	2	Positive	[55]
C. avidum P323	Infant feces	8	2	YEL + M + K	2	Positive	[55]
C. avidum P318	Infant feces	9	1	YEL + M + K	4	Positive	[55]
C. avidum P319	Infant feces	9	1	YEL + M + K	ND[d]	Positive	[55]
C. avidum P330	Infant feces	10	2	YEL + M + K	4	Positive	[55]
C. avidum P313	Infant feces	10	6.5	YEL + M + K	2	Positive	[55]
C. avidum MM2	Breast milk	–	–	Wilkens-Chalgren agar with soy peptone	ND	Positive	Bunesova, unpublished
C. avidum MM12	Breast milk	–	–	Wilkens-Chalgren agar with soy peptone	ND	Positive	Bunesova, unpublished
C. avidum DPC 6544	Infant fecal swab	–	–	–	–	–	[46]
C. avidum MJR7694	Vagina	–	–	–	–	–	[31]
C. avidum TM16	Prostate tissue	–	–	–	–	–	[35]
C. avidum UCD-PD2	Feline anal sac	–	–	–	–	–	[13]
C. avidum T13	Prosthetic joint	–	–	–	–	–	[71]
C. avidum T15	Prosthetic joint	–	–	–	–	–	[71]
C. avidum T14	Prosthetic joint	–	–	–	–	–	[71]
C. avidum CI882	Prosthetic joint	–	–	–	–	Positive[e]	[1]
C. avidum 44067	Skin abscess	–	–	–	–	–	[44]

Strains in bold were used for determination of selected carbon source utilization.
[a] Information not available.
[b] Hemolysis activity was studied using Schaedler agar as described previously [55].
[c] YEL + M + K: yeast extract sodium lactate medium consisting of 1% (w/v) trypticase soy broth without dextrose, 1% (w/v) yeast extract, 117 mM sodium DL-lactate, 0.025% (w/v) KH_2PO_4, 0.0005% (w/v) $MnSO_4$, kanamycin 0.001% (m/v) and metronidazole 0.0004% (m/v).
[d] ND: not determined.
[e] Hemolysis was identified on Brucella agar as described before [1].

predominant *Bifidobacterium* species in early life that are adapted to degrade human milk oligosaccharides (HMO), the major carbohydrate source (5–15 g L^{-1}) in breast milk beside lactose. This activity produces short chain fatty acids (SCFA), monosaccharides and intermediate metabolites (lactate) for cross-feeding [6,8,41]. *B. infantis* and *B. bifidum* use different strategies for uptake and metabolism of HMOs. *B. bifidum* metabolizes HMOs extracellularly by membrane-associated glycosyl hydrolases, releasing monosaccharides, fucose and sialic acid [8,17]. *B. infantis* internalizes mono-, di- and polysaccharides using membrane transporters, before cleavage and intracellular degradation to produce acetate, lactate, formate or ethanol [59]. *Bifidobacterium* can also degrade non-digestible carbohydrates, fructo-oligosaccharides (FOS) and β-galactooligosaccharides (β-GOS), which are used to supplement infant formula [3,7], and mucin, an intrinsic glycan source [9]. Strains of *Cutibacterium* and *Bifidobacterium* spp. could thus cross-feed on monosaccharides and fermentation intermediates, but whether and how *C. avidum* interacts with *Bifidobacterium* spp. has not been investigated to date.

Novel genetic markers such as *glyS*, *infB, rpoB* and *rplB* have been shown to be more suitable for phylogenetic analysis in the *Propionibacteriaceae* family than the 16S rRNA gene [11,40]. Whole genome analysis limited to only a small number of isolates indicated the existence of *C. avidum* subpopulations, as already described for *C. acnes* [11,40]. We were interested in potential evolutionary adaption of *C. avidum* related to habitat selection; thus, we conducted phylogenetic and experimental studies on a collection of *C. avidum* infant isolates. We employed multi-locus sequence analysis (MLSA) based on five novel genetic markers and included *C. avidum* from different niches. Additionally, we investigated the ability of *C. avidum* isolates to degrade and utilize carbon sources available in the infant gut, and also evaluated metabolic cross-feeding between *C. avidum* P279, which was isolated from infant feces [55], and *B. infantis* DSM 20088 and *B. bifidum* BSM 28-1 [67].

Materials and methods

Bacterial strains and growth conditions

Strains used in this study (Table 1) were obtained from the German Collection of Microorganisms and Cell Cultures (DSMZ, Braunschweig, Germany) or from the strain collection of the Laboratory of Food Biotechnology (ETH-Zurich) and the Department of Microbiology, Nutrition and Dietetics, Czech University of Life Sciences, Prague. *C. avidum* infant isolates were obtained from different donors, and diversity was confirmed using rep-PCR and restriction fragment length polymorphism [55]. *C. avidum* were routinely grown in yeast extract sodium lactate medium (YEL) consisting of 1% (w/v) trypticase soy broth without dextrose (Becton Dickinson AG, Allschwil, Switzerland), 1% (w/v) yeast extract (Merck, Darmstadt, Germany), 117 mM sodium DL-lactate 60% syrup (Central Drug House, New Delhi, India), 0.025% (w/v) KH_2PO_4 (VWR International AG, Dietikon, Switzerland) and 0.0005% (w/v) $MnSO_4$ (Sigma-Aldrich, Buchs, Switzerland). *B. infantis* DSM 20088 and *B. bifidum* BSM 28-1 [67] were routinely grown on Wilkens Chalgren medium (WCSP) (Oxoid, Thermo Fisher Diagnostics AG, Pratteln, Switzerland) supplied with 0.5% (w/v) soy peptone (Biolife, Italy), 0.1% (v/v) Tween 80 (Sigma-Aldrich), and

0.05% (w/v) L-cysteine (Sigma-Aldrich). Glycerol stocks stored at −80 °C were reactivated on agar plates and incubated in anaerobic jars (Mitsubishi AnaeroPack, Thermo Fisher Diagnostics AG, Pratteln, Switzerland) containing the AnaeroGen system (Oxoid, Thermo Fisher Diagnostics AG) for 2 (*Bifidobacterium*) or 5 days (*Cutibacterium*) at 37 °C. After incubation, a single colony was picked, transferred into conical polypropylene tubes containing 10 mL of sterile broth and incubated for 24 (*Bifidobacterium*) or 48 h (*Cutibacterium*) at 37 °C. Strains were sub-cultured twice in liquid media before being used as working cultures.

Metabolic cross-feeding between infant isolate *C. avidum* P279 and *B. infantis* DSM 20088 or *B. bifidum* BSM 28-1 was evaluated using modified yeast-extract-casitone-fatty acids medium (Table S1 in Supplementary material) in O_2-free CO_2-sparged Hungate tubes sealed with butyl-rubber stoppers (Dutscher SAS, Brumath, France). Yeast-extract-casitone-fatty acids medium contained 55 mM glucose (mYCFA); lactose (17 mM) and β-GOS (7.2 g L^{-1}) (mYCFA_L- β-GOS) or a mixture of HMOs: 5 mM of each of 2'-fucosyllactose (2'-FL), 3'-fucosyllactose (3'-FL), 3'-sialyllactose (3'-SL), 6'-sialyllactose (6'-SL), and 4.7 mM of LNnT (mYCFA_HMO). To initiate co-culture experiments, working cultures were subcultured once in mYCFA.

Carbon source utilization profile of infant C. avidum *isolates*

To investigate utilization of different carbon substrates, working cultures of *C. avidum* infant isolates (Table 1) and ATCC 25577 were centrifuged at 14,000 *g* for 5 min after 48 h of incubation. The supernatant was discarded, the bacterial pellet was re-suspended in an equal volume of peptone water (Oxoid, Thermo Fisher Diagnostics AG), and 150 μL of the re-suspended pellet were added to conical polypropylene tubes containing 1.5 mL of YEL broth containing different carbon sources in place of sodium-DL-lactate (Table S2 in Supplementary material). YEL without an added carbon source was the control. Cultures were incubated for 48 h at 37 °C. After 48 h, cell growth was assessed by measuring optical density at 600 nm (OD_{600}). Concentrations of substrate, SCFA and intermediate metabolites in the supernatant were determined by high-pressure liquid chromatography analysis with refractive index detection (HPLC-RI; detailed below). Unless otherwise indicated, carbon utilization and metabolite formation were assessed for each strain in independent triplicates, and in duplicates for control fermentations and HMO-mix.

Enzymatic activity of infant and breast milk C. avidum *isolates*

Enzymatic activity profiles of *C. avidum* ATCC 25577 and 18 *C. avidum* infant feces and breast milk isolates were investigated using API ZYM system (bioMérieux SA, Geneve, Switzerland). Cupules in each strip were filled with 130 μL of 48 h working cultures in duplicate, and were incubated according to manufacturer's instructions. For reaction evaluation, scores were ranked visually from 0 to 3 (0 = no reaction, 3 = strong reaction).

Single and co-culture growth of C. avidum *P279 and* B. infantis *DSM 20088 or* B. bifidum *BSM 28-1*

To inoculate single culture experiments, 100 μL of each of *C. avidum* P279, *B. infantis* DSM 20088 and *B. bifidum* BSM 28-1 cultures grown in mYCFA were transferred to each of the test media (mYCFA_L-β-GOS and mYCFA_HMO, each 9 mL) and incubated for 24 h at 37 °C. For co-cultures, 100 μL of *C. avidum* P279 and 100 μL of *B. infantis* DSM 20088 or *B. bifidum* BSM 28-1 cultures were transferred into the same Hungate tube containing each test medium (9 mL) and were incubated at 37 °C. Samples (500 μL) were collected at 0, 4, 8, and 24 h, centrifuged, and supernatants and cell mass were stored at −20 °C for later analysis. Metabolic cross-feeding in mYCFA_L-β-GOS was performed in independent biological triplicates and in independent biological duplicates for mYCFA_HMO.

HPLC analysis with refractive index detection (HPLC-RI)

Concentrations of fucose, glucuronic acid, lactose, acetate, propionate, butyrate, formate, succinate and lactate were determined in the supernatant. Supernatant (500 μL) was filtered through a 0.45 μm membrane (Millipore AG, Zug, Switzerland) into glass HPLC vials (Infochroma, Hitachi LaChrome, Merck, Dietikon, Switzerland) and sealed with crimp-caps. An HPLC (Hitachi LaChrome) equipped with a Security Guard Cartridges Carbo-H column (4 × 3 mm; Phenomenex Inc., Torrance, CA, USA), a Rezex ROA-Organic Acid H+ column (8%, 300 × 7.8 mm; Phenomenex) and a refractive index detector (HPLC-RI) was used. The column was eluted with 10 mM H_2SO_4 (Fluka, Buchs, Switzerland) as mobile phase at a flow rate of 0.4 mL min^{-1} at 25 °C. Fucose, glucuronic acid, succinate, SCFA and lactate were quantified using external standards.

Analysis of HMO, maltodextrins, α- and β-GOS degradation using high performance anion exchange chromatography with pulsed amperometric detection (HPAEC-PAD)

Degradation of oligosaccharides was investigated using HPAEC-PAD on a Dionex IC3000 equipped with a CarbopacPA20 column (Thermo Fisher Diagnostics AG) and an electrochemical detector with a gold electrode. Water (A), 200 mM NaOH (B), and 1 M Na-acetate (C) were used as solvents at a flow rate of 0.25 mL min^{-1}. For HMO separation, a gradient of: 0 min 30.4% B, 1.3% C, 22 min 30.4% B, and 11.34% C followed by washing and regeneration was applied. HMO, sialic acid and L-fucose were identified using external standards, and either utilization or accumulation were semi-quantitatively assessed as fold change of the area under the curve at t = 24 h compared to time 0.

DNA isolation from C. avidum *infant isolates*

Genomic DNA from *C. avidum* infant isolates used for MLSA and whole-genome sequencing (Table 1) was extracted from the working culture (2 mL) using the Wizard genomic DNA purification kit (Promega AG, Switzerland) following the manufacturer's instructions. Genomic DNA from *C. avidum* breast milk isolates used for 16S rRNA and MLSA sequencing was extracted from the working culture (1 mL) using PrepMan® Ultra Sample Preparation Reagent protocol (Thermo Fisher Scientific, Waltham, MA, USA). The DNA concentration was measured using a NanoDrop ND-1000 Spectrophotometer (Witec AG, Littau, Switzerland). DNA quality was analysed by electrophoresis using a 1% (w/v) agarose gel, stained in a GelRed staining bath (Biotium Inc., Hayward, CA, USA) and visualized using UV light. DNA was stored at −20 °C until further analysis.

Multilocus sequence analyses (MLSA)

Overall, 28 strains of *C. avidum* were included for the genotyping analysis based on five housekeeping genes (*glyS*, *infB*, *rplB*, *groEL* and *pyrG*) (Table S3 in Supplementary material); for 10 strains, gene sequences were obtained from the complete genomes deposited in the NCBI database (https://www.ncbi.nlm.nih.gov/nuccore/). The sixteen *C. avidum* infant strains had been previously typed to species level using 16S RNA gene sequences and further compared to NCBI database and evaluated for hemolytic activity (Table 1) [55]. The two breast milk isolates (MM2 and MM12)

were identified by sequence analysis of the almost complete 16S rRNA gene sequences. The closest relative species to both isolates, whose sequences were deposited in the NCBI database under the numbers MK386898 (strain MM2) and MK386899 (strain MM12), was *C. avidum* ATCC 25577^T with 99.8% 16S rRNA gene similarity in 1364 and 1389 bp, respectively (Table S3 in Supplementary material). PCR conditions and specific primers for amplification of variable fragments of the *glyS*, *infB* and *rplB* genes were used as described recently [40]. Primers flanking the desired fragments of *groEL*, encoding the chaperon protein groEL/60 kDa heat shock protein (912 bp, positions 231,859,1–231,950,2 in genome of *C. avidum* DPC 6544, accession number CP016954) and *pyrG*, encoding the CTP synthase (579 bp, positions 399,88–405,66 in genome of *C. avidum* DPC 6544), were designed based on gene sequences of *Acidipropionibacterium acidipropionici*, *Acidipropionibacterium jensenii*, *Cutibacterium acnes* subsp. *acnes*, *C. avidum*, *C. granulosum* and *Propionibacterium freudenreichii* subsp. *freudenreichii* type strains (Table S3 in Supplementary material). These genes were identified as suitable classification and phylogenetic markers in previous studies [19,23,25]. Specific primers and PCR conditions are shown in Table S4 in Supplementary material. The proposed gene regions contained no indels.

Phylogenetic analysis was performed based on the Akaike Information Criterion (AIC) best fit maximum-likelihhood (General Time Reversible + Gamma distributed rates among sites) method and bootstrap improvement (1000 replicates) in the MEGA v6.0 software package [64]. The gene concatenate of *glyS* (678 bp), *infB* (846 bp), *rplB* (549 bp), *groEL* (912 bp) and *pyrG* (579 bp) aligned using ClustalW [40] served as an input file for reconstruction. Phylogenetic reconstruction was completed by six representatives of the *Propionibacteriaceae* family (Table S3 in Supplementary material) to increase the accuracy of the topology. The tree was rooted by *P. freudenreichii* subsp. *freudenreichii* type strain. As illustrated in Fig. 1 and calculated using the eBURST application [26], 15 different STs (sequence types) in concatenated sequences were revealed among 18 strains (the same sequences were determined only in strain pairs P315–P336 and P313–P330 and MM2–MM12) of *C. avidum* isolated from infant feces and breast milk. To identify subpopulations, a sequence identity matrix was generated based on the concatenated sequences using the tool implemented in BioEdit, and a cut-off value of 98.9% was employed. Phylogenetic reconstructions based on individual gene alignments were carried out according to the same procedure outlined above.

Sequences are available at GenBank (NCBI) under the accession numbers listed in Table S3 in Supplementary material.

Genome analysis

We generated the draft genome of *C. avidum* P313 to validate phenotypic analysis. Genome libraries of *C. avidum* P313 were sequenced with an Illumina MiSeq to obtain paired-end reads of 2 × 150 bp. Sequencing was conducted at the Functional Genomic Center Zürich (FGCZ, ETH-Zürich, Zürich, Switzerland). The genome was assembled using Abyss v.1.9.0 for paired-end libraries implemented in Bio-Linux 8. The partial genome was functionally annotated with RAST using default settings [4]. Average nucleotide identity (ANI) was calculated using an online tool [56]. Available genomes of *C. avidum* strains (Table S3 in Supplementary material) were also uploaded to RAST and screened for β-glucuronidase- and α-galactosidase-encoding genes. Glycosyl hydrolases were identified using the dbCAN database based on a search for signature domains of every CAZyme family [74]. The assembled genome contigs are available under BioProject ID PRJNA524452.

DNA isolation from single- and co-cultures and quantitative PCR analysis (qPCR)

Genomic DNA was extracted from bacterial pellets using the Fast DNA SPIN kit for soil (MP Biomedicals, Illkirch, France) according to manufacturer's instructions. Reactions were performed using a 7500 Fast Real-Time PCR System (Applied Biosystems, Zug, Switzerland), 2 × Kappa SYBR FAST qPCR mastermix and 0.2 μM primers (Biolab Scientifics Instruments SA, Chatel-St-Denis, Switzerland). Thermal cycling started with an initial denaturation step at 95 °C for 3 min, followed by 40 cycles of denaturation at 95 °C for 3 s, annealing at 60 °C for 10 s, and elongation at 72 °C for 25 s. To generate standards, 16S rRNA gene PCR amplicons from *C. avidum* ATCC 25577 (1445 bp) and *B. adolescentis* DSM 20083 (1451 bp) were cloned into the pGEM-T Easy Vector and heterologously expressed in *E. coli* according to instructions of the supplier (Promega AG, Dübendorf, Switzerland). Standard curves were prepared from ten-fold dilutions of linearized plasmids harboring the target gene of interest. *C. avidum* P279 was quantified using primers avi_fwd (5'-GTCTGCAACTCGACCCCAT-3') and avi_probe (5'-CTTCGACGGCTCCCCCACACAGGT-3') [55], while *B. infantis* and *B. bifidum* were quantified using primers bif_F (5'-TCGCGTCYGGTGTGAAAG-3') and bif_R (5'-CCACATCCAGCRTCCAC-3') [54]. Melting curve analysis was conducted to confirm specificity. The linear detection range was between 1.3 and 7.3 log gene copies for *C. avidum* and 2.5 and 7.5 log gene copies for bifidobacteria, primer efficiency was 91 and 105%, respectively. Log gene copies were corrected for multiple copies of 16S rRNA genes for *C. avidum* (n = 3), *B. infantis* (n = 4) and *B. bifidum* (n = 3) to calculate cell number [8,63].

Statistical analysis

Statistical analyses were done using SigmaPlot (Systat Software, San Jose, CA, USA) with statistical significance set at a *p*-value of less than 0.05. Correlation between propionate produced in YEL with α-GOS and α-galactosidase activity of isolates was calculated using Pearson's correlation coefficient. The Student's t-test with two-tailed distribution was used after testing for normal distribution using the Shapiro-Wilk test to identify significant differences in growth (log cells mL^{-1} detected by qPCR) and metabolite formation and/or consumption of carbohydrates between single and co-cultures in mYCFA_L-β-GOS.

Results

Phylogenetic diversity of C. avidum *isolates from infant feces and other sources*

C. avidum strains have been repeatedly isolated and identified in infant feces, but their phylogenetic relationship to isolates from other body sites remains unclear. An extended MLSA screening using five housekeeping genes (*glyS*, *infB*, *rplB*, *pyrG* and *groEL*) as markers showed genetic heterogeneity within *C. avidum* isolates. This genetic heterogeneity was also confirmed when individual genes were used for tree construction (Figures S5–S9 in Supplementary material), however, with individually varying topologies. MLSA screening based on concatenated sequences identified a group of *C. avidum* strains that were delineated by a similarity threshold of 99.3 ± 0.3% similar (Fig. 1). This group included various isolates from infant feces including strain DPC 6544 together with strain UCD-PD2 isolated from a feline anal sac [13,46]. Most isolates of this subpopulation were non-hemolytic. The similarity of this subpopulation to other strains such as TM16, isolated from human prostate tissue [36], the type strain ATCC 25577 isolated from the

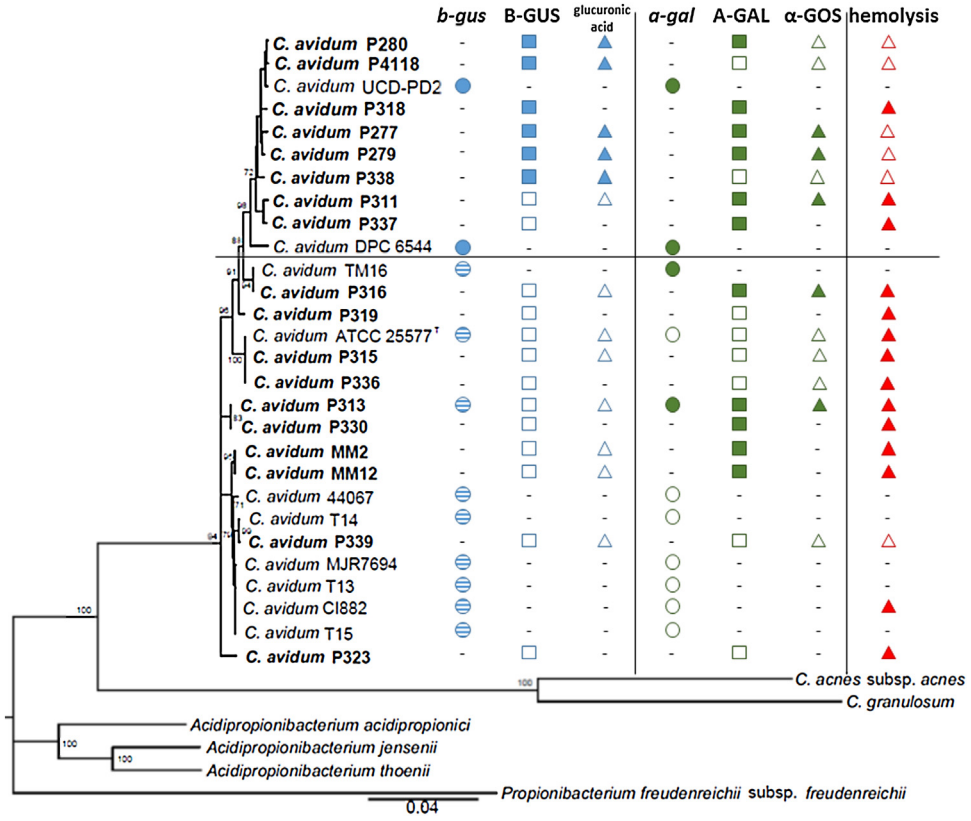

Fig. 1. Phylogenetic tree based on concatenated nucleotide sequences derived from five genes (*glyS, infB, rplB, pyrG* and *groEL*) and genotypic and phenotypic features of *C. avidum* strains.
Genomes of available *C. avidum* strains were screened for genes (*b-gus*, *a-gal*) encoding for β-glucuronidases (B-GUS) and α-galactosidases (A-GAL) using RAST. Beta-glucuronidase and α-galactosidase enzymatic activity were detected using the chromogenic and semi-quantitative API-ZYM. Consumption of glucuronic acid and α-GOS by selected strains were evaluated during growth in YEL medium supplied with the respective carbohydrates. Concatenated nucleotide sequences from **s**trains above the horizontal line were 99.3 ± 0.3% similar. Full symbol: positive; empty symbol: negative; circles with horizontal pattern indicate that *b-gus* was incomplete; -: not determined. Strains in bold were included for phenotypic tests in this study.

oral cavity [44], to infant fecal isolates P313, P315, P316, P319, P323, P330, P336 and P339, two breast milk isolates (MM2 and MM12), one vaginal strain (MJR7694), four isolates from infected prosthetic joints (CI882, T13, T14 and T15) and a strain obtained from a skin abscess (44067) [1,31,44,71] was 98.1 ± 0.4% (Table S5 in Supplementary material). Strains P338 and P339 were originally isolated from the same donor, confirming previous observations that infants carry more than one strain [55].

Fermentation of monosaccharides and glycerol by C. avidum *strains*

To investigate the ability of infant isolates and *C. avidum* ATCC 25577 to use glycerol and monosaccharides derived from microbial cross-feeding, we assessed growth, substrate utilization and metabolite production in YEL supplemented with selected carbon sources after 48 h of incubation.

Background growth was observed in YEL without added carbon (OD_{600} 1.6–2), together with production of SCFA (11.4–27.4 mM propionate and 6.6–11.2 mM acetate) and a decrease of pH from 7.0 to 6.1 after 48 h incubation (Table 2 and S6 in Supplementary material). All tested *C. avidum* isolates were able to grow in the presence of sodium-DL-lactate (consumption between 64.4–124.3 mM) and in 85 mM potassium-L-Lactate (complete degradation), producing a mean propionate:acetate ratio of 2.1 ± 0.2 (Table S6 in Supplementary material) as previously reported [72].

All strains showed a high capacity to ferment glucose, galactose and GlcNAc (Table S6 in Supplementary material). Glucose was consumed by all strains, with P316 and P338 producing 2 mol propionate and 1 mol of acetate from 1.5 mol glucose, as expected from Embden-Meyerhof-Parnas (EMP) pathway [72]. Interestingly, this theoretical yield was different for all other infant strains, which produced only 1.2 ± 0.2 mol propionate and 0.5 ± 0.1 mol acetate for every 1.5 mol of glucose consumed. Galactose consumption was observed (15.8–33.9 mM) by most strains tested, accompanied by high biomass production (OD_{600} 2.8–5.4) and a decrease in pH to 4.3. GlcNAc was also used (13.5–46.5 mM), leading to the release of the acetyl residue (Table S6 in Supplementary material).

All tested *Cutibacterium* strains degraded glycerol with 0.8 ± 0.1 mol of propionate produced from one mol glycerol consumed (Table S7 in Supplementary material). This yield was coincidental with the theoretical yield obtained via the EMP pathway (production of 1 mol propionic acid and no acetic acid for each mol of glycerol) [69]. High biomass production (OD_{600} 3.2–5.1) and a final pH of 4.6 were observed. In agreement with previous observations for *Propionibacterium freudenreichii* subsp. *shermanii,* glycerol was preferred over glucose by *C. avidum* strains (Table S7 in Supplementary material) [69]. In contrast, no growth on fucose was observed for all *C. avidum* strains (Table 2).

C. avidum *showed variable capability of degrading and consuming di- and oligosaccharides*

To investigate the ability of *C. avidum* infant and breast milk isolates and ATCC 25577 to degrade di- and oligosaccharides, we assessed hydrolytic activity using the chromogenic and semi-

Table 2
Growth, carbon utilization and metabolite formation of *C. avidum*. Growth and substrate utilization of type strain and infant isolates (n = 10) was investigated using YEL media supplemented with selected carbon sources and compared to the control without carbon source. Carbon utilization and SCFA production (mM) was assessed in independent triplicates for each strain except for growth tests in control medium for which only duplicates were evaluated. ND: not determined.

YEL supplemented with	Strains	Carbon source consumed		Propionate		Acetate		Propionate/acetate		OD_{600}	
		Mean	SD	Mean	SD	Mean	SD	Mean	SD	Mean	SD
Control	ATCC 25577			9.8		6.5		1.5		1.5	
	Mean infant isolates			20.4 ±	4.8	9.7 ±	1.6	2.1 ±	0.3	1.9 ±	0.3
DL- Lactate (126 mM)	ATCC 25577	−88.4 ±	0.2	72.8 ±	3.3	35.6 ±	2	2 ±	0	2.9 ±	0.2
	Mean infant isolates	−90.8 ±	16.7	72.1 ±	18.2	31.8 ±	7.7	2.3 ±	0.1	3 ±	0.7
K-Lactate (85 mM)	ATCC 25577	−85.9 ±	0	62.3 ±	7.1	32.2 ±	3.8	1.9 ±	0	2 ±	0
	Mean infant isolates	−85.4 ±	1.4	61.3 ±	11.8	31.5 ±	2.5	2 ±	0.4	2.8 ±	0.5
Lactose (55 mM)	ATCC 25577	−9.4 ±	0.5	13.2 ±	0.3	7.0 ±	0.4	1.9 ±	0.1	1.9 ±	0.1
	Mean infant isolates	−11.1 ±	6	19.9 ±	6	9.4 ±	1.5	2.1 ±	0.5	2.8 ±	0.8
Glucose (111 mM)	ATCC 25577	−35 ±	0.6	25.8 ±	0.6	13.4 ±	0.5	1.9 ±	0.1	2.3 ±	0.1
	Mean infant isolates	−38.5 ±	7.9	33.4 ±	10.4	14 ±	3.9	2.4 ±	0.4	3.4 ±	1
Galactose (102 mM)	ATCC 25577	−26.3 ±	2.5	27.9 ±	1	15.3 ±	0.1	1.8 ±	0.1	3.9 ±	0
	Mean infant isolates	−22.1 ±	4.5	21.6 ±	7.7	12.5 ±	2.5	1.6 ±	0.6	3.3 ±	0.4
N-acetyl-D-glucosamine (93 mM)	ATCC 25577	−25.3 ±	7	45.5 ±	2	79.3 ±	4.1	0.6 ±	0	3.1 ±	1.1
	Mean infant isolates	−29.3 ±	11.3	43.1 ±	11.2	57 ±	20.6	0.9 ±	0.8	3.3 ±	0.8
D-Glucuronic acid (60 mM)	ATCC 25577	−4.1 ±	0.3	7.9 ±	1.1	5.3 ±	0.1	1.5 ±	0.2	1.6 ±	0.1
	Mean infant isolates	−31 ±	26.4	27.6 ±	17.9	27.3 ±	22.1	1.3 ±	0.5	4.5 ±	3
Glycerol (122 mM)	ATCC 25577	−51.1 ±	0.5	35.3 ±	0.6	1.9 ±	0.2	18.6 ±	1.8	1.8 ±	0
	Mean infant isolates	−73.7 ±	5.4	57.6 ±	7.6	2.2 ±	0.8	30 ±	13.4	3.7 ±	0.6
α- GOS	ATCC 25577	ND		5.1 ±	0.2	5.4 ±	0.2	0.9 ±	0	1.1 ±	0
	Mean infant isolates	ND		23.5 ±	11.9	12.8 ±	5.4	1.8 ±	0.3	2.6 ±	1.2
Maltodextrin	ATCC 25577	ND		16 ±	0.4	8.8 ±	0.2	1.8 ±	0	2.7 ±	0.1
	Mean infant isolates	ND		23.1 ±	4.4	9.9 ±	1.3	2.3 ±	0.4	3.1 ±	0.3
β-GOS	ATCC 25577	ND		8.9 ±	0.3	6.5 ±	0.4	1.4 ±	0.1	1.3 ±	0
	Mean infant isolates	ND		17.5 ±	6.1	8.9 ±	1.4	1.9 ±	0.5	1.7 ±	0.1
FOS	ATCC 25577	ND		6.6 ±	0.1	7 ±	0.1	0.9 ±	0	1.1 ±	0
	Mean infant isolates	ND		13.3 ±	4.2	7.7 ±	1.1	1.7 ±	0.5	1.5 ±	0.1
Fucose (107 mM)	ATCC 25577	ND		6 ±	0.3	8 ±	0.1	0.8 ±	0	1.1 ±	0.1
	Mean infant isolates	ND		9.8 ±	3.2	9.5 ±	1.6	1 ±	0.3	1.2 ±	0.2

quantitative API-ZYM test, and conducted growth studies providing the relevant di- and oligosaccharides as substrates.

All strains possessed medium to high β-galactosidase activity (Table S8 in Supplementary material), and thus were potentially capable of hydrolyzing lactose and β-GOS. Beta-GOS have a degree of polymerization of 2–6 units and contain β1-3, -4 or -6 linkages [65]. Lactose utilization was variable, ranging from 3 to 17.2 mM (Table S9 in Supplementary material). Minor changes in β-GOS profiles indicated that *C. avidum* had a limited capacity to use β-GOS (Figure S1 and Table S9 in Supplementary material).

All strains were positive for α-glucosidase (Table S8 in Supplementary material). We tested growth using maltodextrins, which are linear α1-4-linked D-glucose polymers with some α1-6 branching points, as substrate. All infant isolates grew in the presence of maltodextrins, reaching OD_{600} 2.7–3.5 (Table S9 in Supplementary material) and degrading oligosaccharides up to a chain length of 10 glucosyl units (Figure S2 in Supplementary material).

The activity of α-galactosidase, which hydrolyses Gal-α1-6 bonds of galacto-oligosaccharides from the raffinose family (α-GOS), varied between isolates (Table S9 in Supplementary material). Infant isolates P311, P279, P277, P316 and P313 showed highest turbidity and SCFA production compared to all other strains when grown in YEL with α-GOS. Final OD_{600} was positive correlated with α-galactosidase activity in the API ZYM test ($R = 0.8$; $p = 0.003$), with the exception of P280. The increase in biomass (OD_{600}) and SCFA concentrations corresponded with degradation of the supplied α-GOS (Figure S3 in Supplementary material).

Activity of β-glucuronidase, which releases the terminal glucuronic acid from glucuronated metabolites, was detected in the non-hemolytic strains P4118, P279, P280, P277, P338 and P318 (Table S8 in Supplementary material). Strains exhibiting β-glucuronidase activity were able to ferment glucuronic acid into propionate and acetate in 1:1 ratio. Weak growth and no metabolism of glucuronic acid was observed for strains negative for β-glucuronidase activity (Table S6 in Supplementary material).

FOS (Table S9 in Supplementary material) or HMOs (data not shown) were not degraded by *C. avidum* isolates, and turbidity and metabolite production observed were similar to growth in YEL without added carbohydrates (Table 2).

Genomic potential of C. avidum *to hydrolyse selected di-and oligosaccharides*

To validate the phenotypic analysis, we generated the draft genome of *C. avidum* P313 and also examined publically available genomes (Table S10 in Supplementary material). Abyss assembly yielded 48 contigs (>200 bp). The ANI of P313 was 96.23% compared to *C. avidum* DPC 6544 (GenBank accession no. CP016954.1) and 98.41% compared to *C. avidum* 44067 (GenBank accession no. CP005287.1). In agreement with phenotypic analysis, P313 had limited capacity to degrade di-, oligo- and polysaccharides and glycosylated compounds, as indicated by the presence of genes encoding only α- and β-galactosidases, α- and β-mannosidases, and α-glucosidases (Table S10 in Supplementary material). Because the distribution of active α-galactosidases and β-glucuronidases was limited to some phylogenetic clades (Fig. 1), we additionally screened available *C. avidum* genomes for the presence of the corresponding genes. Genes encoding β-glucuronidases were observed in all strains; however, only DPC 6544 and UCD-PD2 possessed presumptive full-length proteins. ATCC 25577, T13, T15, Cl882 and P313 harboured genes encoding nearly full length proteins with an internal ORF gap of about 27 AA (position 323–350), while the partial β-glucuronidases of T14, TM16 and MJR694 additionally lacked the first N-terminal 190 AA. In agreement with the fragmented structure of the β-glucuronidase of ATCC 25577 and P313, there was no activity observed in the API ZYM test (Fig. 1). The full length β-glucuronidase of DPC 6544 had the highest homology to

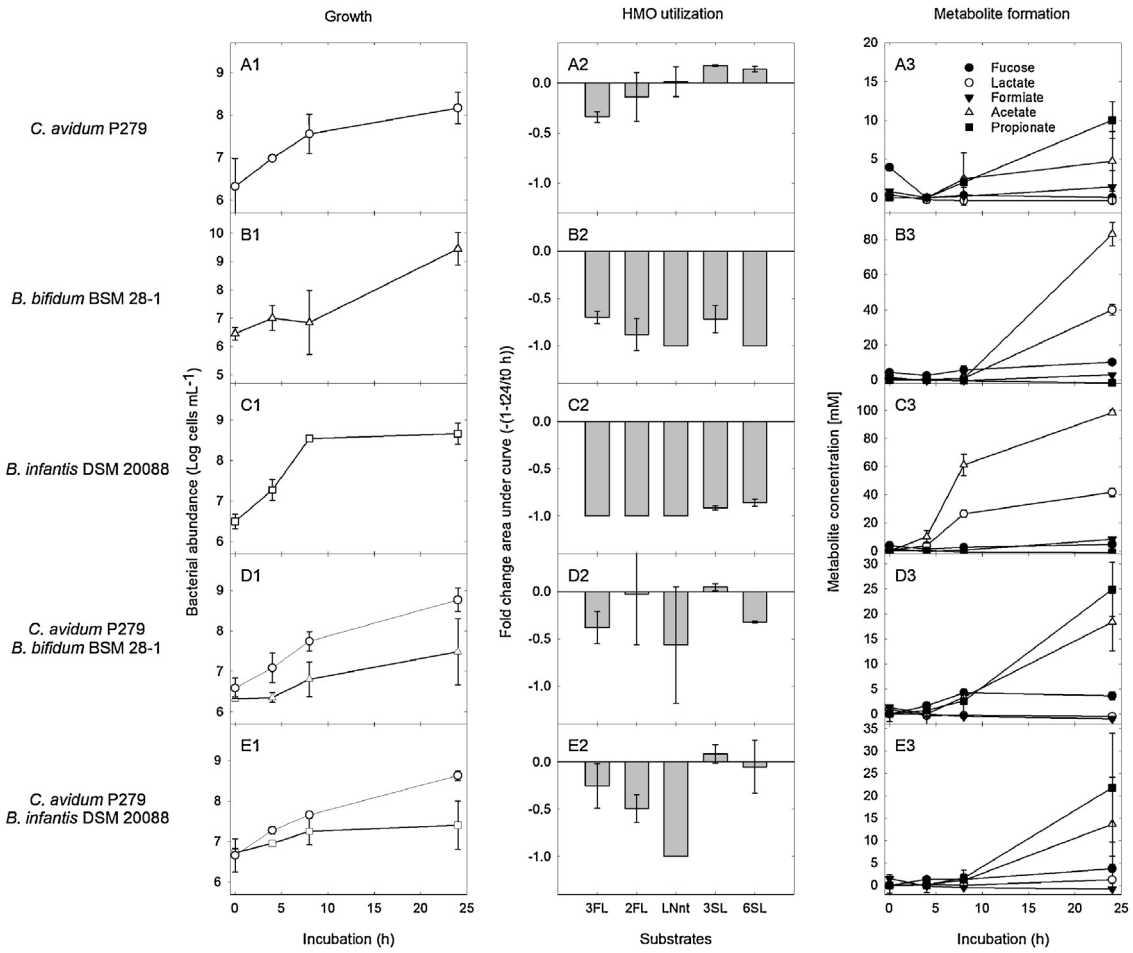

Fig. 2. Growth and metabolism of single- and co-cultures in mYCFA_HMO.
Strain abundance (A1-E1) and HMOs utilization after 24 h of incubation (A2-E2), and metabolite formation (A3-E3) of *C. avidum* P279 (A), *B. bifidum* BSM 28-1 (B), *B. infantis* DSM 20088 (C), *C. avidum* P279/*B. bifidum* BSM 28-1 co-culture (D), and *C. avidum* P279/*B. infantis* DSM 20088 co-culture (E) in mYCFA_HMO during incubation at 37 °C. Mean values and standard deviations from two independent experiments are shown.

partial or full length β-glucuronidases from other *C. avidum* with available genomes (98–100% homology), to β-glucuronidase of *C. acnes* (84–86%), and less than 65% homology to β-glucuronidases of other Actinobacteria such as *Intrasporangium* and *Pseudosporangium* spp. and *Georgenia muralis*. Interestingly, genes encoding for β-glucuronidases in strains DPC 6544, UCD-PD2, 44067, T14, MJR 694 and TM 16, were located in close proximity to genes encoding a glucuronide transporter *uidB*, urinate isomerase, mannoate-dehydrogenase and mannoate–oxidoreductase, which are all presumably involved in glucuronate utilization (Figure S4 in Supplementary material). An enzyme characteristic of the Entner-Doudoroff (ED) pathway, 2-dehydro-3-deoxyphosphogluconate aldolase, was also detected in the genomes of strains encoding genes related to glucuronic acid utilization, but in other locations in the genome. In DPC 6544 and UCD-PD2, an α-glucosidase was located adjacent to the β-glucuronidase-encoding genes. Genes encoding for α-galactosidases were present in DPC 6544, UCD-PD2, and TM16 (Fig. 1). *C. avidum* α-galactosidases had the highest homology to each other (98–100% homology) and less than 60% homology to α-galactosidases of *A. jensenii* and other Actinobacteria such as *Brachybacterium* spp.

Growth and cross-feeding of C. avidum *P279 and* B. infantis *or* B. bifidum *in mYCFA supplemented with HMO*

Our results indicated that infant *C. avidum* isolates metabolised glucose, galactose and GlcNAc, which are constituents of HMOs and β-GOS, and also the fermentation intermediate lactate. We therefore assessed cross-feeding between *C. avidum* P279 and *B. infantis* or *B. bifidum* in co-culture in mYCFA supplemented with HMOs (4.7 mM of LNnt and 5 mM of each 2′-FL, 3′-FL, 3′-SL and 6′-SL) or with lactose (17 mM) and β-GOS (7.2 g L^{-1}) (Table S1 in Supplementary material) by comparing with single cultures of each strain.

Single cultures in mYCFA HMO were inoculated with similar initial levels for each strain (differences below log 0.2 cells mL^{-1}) (Fig. 2A1, B1 and C1). *C. avidum* P279 reached a cell concentration of log 8.2 cells mL^{-1} after 24 h of incubation and produced 10.0 mM of propionate and 4.7 mM of acetate, which could result from metabolism of peptides and/or from partial degradation of 3′-FL (reduction of 34% at 24 h) (Fig. 2 A1–3). Single cultures of *B. bifidum* reached a higher cell density of log 9.4 cells mL^{-1} and consumed all the added HMOs after 24 h, with accumulation of fucose (10.1 mM) and sialic acid (semi-quantitatively assessed), and production of acetate (83.1 mM), lactate (40.0 mM) and formate (2.9 mM) (Fig. 2B1–3). *B. infantis* consumed all HMOs, and reached log 8.7 cells mL^{-1} after 24 h of incubation, with production of acetate (98.5 mM), lactate (41.7 mM) and formate (8.3 mM) and residual fucose (4.8 mM). *B. infantis* released only 1/5 of the sialic acid released by *B. bifidum* (Fig. 2C1–3).

When *C. avidum* P279 was grown in mYCFA_HMO with either *B. infantis* or *B. bifidum*, *C. avidum* reached higher cell numbers (log 8.6 and 8.8 cells mL^{-1}, respectively) than in single cultures, whereas bifidobacteria yielded lower cell numbers (log 7.4 cells mL^{-1} for

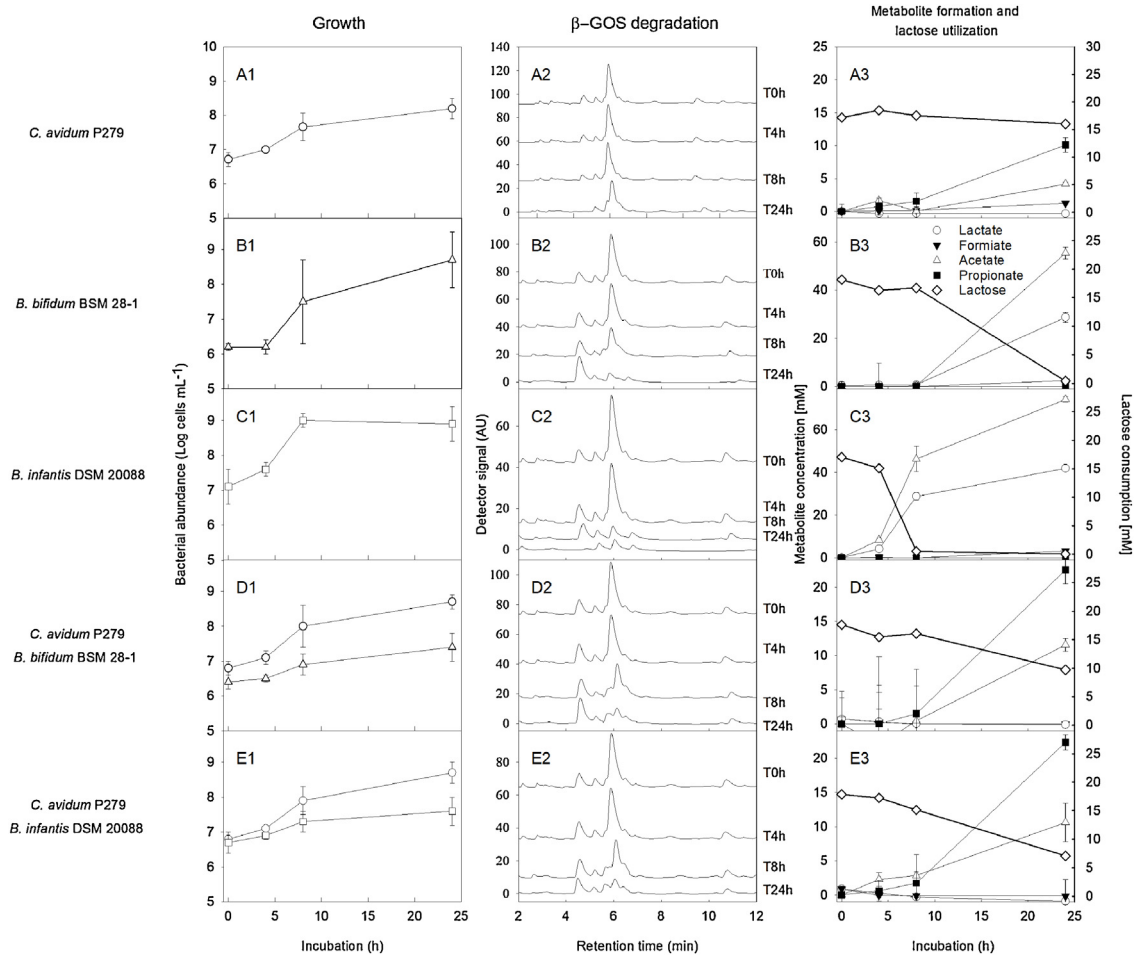

Fig. 3. Growth and metabolism of single- and co-cultures in mYCFA_L-β-GOS.
Strain abundance (A1–E1), β-GOS degradation (A2-E2), metabolite formation and lactose utilization of infant isolate *C. avidum* P279 (A), *B. bifidum* BSM 28-1 (B), *B. infantis* DSM 20088 (C), *C. avidum* P279/*B. bifidum* BSM 28-1 co-culture (D), and *C. avidum* P279/*B. infantis* DSM 20088 co-culture in mYCFA_L-β-GOS during incubation at 37 °C. Mean values and standard deviations from three independent experiments are shown.

B. infantis and log 7.5 cells mL^{-1} for *B. bifidum*) (Fig. 2D1 and E1). *B. infantis* consumed 50% of 2′-FL, 25% of 3′-FL and 5% of 6′- SL to produce propionate (21.8 mM) and acetate (13.7 mM) with residual fucose (3.7 mM) (Fig. 2E1–3). *B. bifidum* degraded 38% of 3′-FL, 2% of 2′-FL, 57% of LNnt and 32% of 6′- SL, and accumulated fucose (3.7 mM), and lactose and/or disaccharides (8.5 mM) eluting with the same retention time (Fig. 2D1–3). Compared to single cultures of *C. avidum* P279 there was more propionate (24.9 mM) and acetate (18.4 mM) produced during co-cultures with *B. bifidum*.

Growth and cross-feeding of C. avidum *P279 and* B. infantis *or* B. bifidum *in mYCFA supplemented with lactose and β-GOS*

Growth and metabolite production of *C. avidum* P279 in mYCFA_HMO and mYCFA_L-β-GOS (log 8.2 ± 0.3 cells mL^{-1}, 10.1 ± 1.4 mM propionate and 4.1 ± 3.1 mM acetate) were similar. Lactose and β-GOS were not utilized by *C. avidum* P279 (Fig. 3A1–3). In contrast, *B. infantis* reached a higher cell concentration (log 8.9 ± 0.5 cells mL^{-1}) with nearly complete degradation of lactose (17.0 ± 0.2 mM, retention time at approximately 6 min) and β-GOS after 24 h incubation, producing acetate (74.1 ± 1.3 mM), lactate (41.9 ± 0.1 mM) and formate (3.2 ± 0.4 mM) (Fig. 3C1–3). Because the theoretical yield of the bifid shunt is 3 mol of acetate and 2 mol of lactate for 1 mol of lactose [20], it may be estimated that approximately one-third of the acetate and lactate were produced from β-GOS utilization. *B. bifidum* grew to log 8.7 ± 0.8 cells mL^{-1} and completely hydrolyzed lactose and degraded β-GOS during 24 h incubation, which resulted in the production of acetate (55.4 ± 2.4 mM), lactate (28.2 ± 2.0 mM) and formate (2.4 ± 0.7 mM) and the accumulation of galactose (2.8 ± 0.7 mM) (Fig. 3B1–3).

Cell densities of *C. avidum* P279 in mYCFA_L-β-GOS co-cultures with *B. infantis* (log 8.7 ± 0.3 cells mL^{-1}) and *B. bifidum* were similar (log 8.7 ± 0.2 cells mL^{-1}) and not significantly different from the single culture ($p = 0.09$ and $p = 0.1$, respectively). The growth of *B. infantis* (log 7.6 ± 0.4 cells mL^{-1}) and *B. bifidum* (log 7.4 ± 0.4 cells mL^{-1}) was inhibited in co-cultures with *C. avidum* P279 (significantly for *B. infantis*; $p = 0.03$) compared to single cultures, despite similar initial cell concentrations (Fig. 3D1 and E1). During co-cultures, propionate production (22.3 ± 1.1 mM and 22.5 ± 2.0 mM for *B. infantis* and *B. bifidum*, respectively) was significantly enhanced compared to single culture of *C. avidum* P279 (10.1 ± 1.4 mM; $p < 0.01$). Bifidobacteria partially consumed lactose (7.9 ± 0.5 mM and 10.8 ± 0.8 mM for *B. bifidum* and *B. infantis*, respectively) and β-GOS (Fig. 3D–E). Formation of acetate was similar for both bifidobacteria, with 11.6 ± 1.0 mM (*B. bifidum*) and 10.6 ± 2.8 mM (*B. infantis*). Galactose accumulated (3.8 ± 0.2 with *B. infantis* and 3.1 ± 1.5 with *B. bifidum*), while formate was not detected in co-cultures (<1.0 mM) (Fig. 3D1–3 and E1–3).

Discussion

In this study, we examined whether infant *C. avidum* strains are adapted to the infant gut environment. We thereby combined two approaches: for all strains with available isolates, we determined enzyme activity and for all strains with available genomes, we determined the potential for β-glucuronidase and α-galactosidase activity (= presence of enzyme encoding genes). Alpha-galactosidase and β-glucuronidase activity were variable between strains and most prominent in a phylogenetically closely related group, which harbored mostly strains isolated from infant fecal samples, suggesting these two functions as ecological adaptive traits. *C. avidum* strains isolated from infant feces had the ability to produce propionate and acetate through cross-feeding with bifidobacteria.

C. avidum *are genetically heterogeneous and a subpopulation might be adapted to the infant gut environment*

C. avidum strains were genetically heterogeneous, nevertheless we identified a group of strains, which was almost exclusively represented by isolates from infant feces. Further infant isolates grouped together with strains from different body sites suggesting niche adaptation by a subpopulation of *C. avidum*. In agreement with two previous analyses based on whole genome orthoANI and on single-nucleotide polymorphisms in the core genomes of different *C. avidum* strains, our analysis identified UCD-PD2 and DPC 6544 as different subpopulations from the type strain ATCC 25577 [1,11].

Specific enzymatic activity may confer niche adaption

Cutibacterium species have adapted to specific niches by acquiring genes encoding for specific metabolic traits e.g. carbohydrate transporters and lipases, and losing functions e.g. branched-chain amino-acid transporters [35,58]. Proteolytic activity and preference for humid skin regions, together with mutualistic colonization in areas rich in enteric Gram-negative bacteria, have been suggested as adaptive traits specific of *C. avidum* [11].

In the infant gut ecosystem, the ability to use carbohydrates as energy sources provides a competitive advantage. While all tested strains were able to use maltodextrins and lactose, highlighting the ability to utilize starch-like dietary compounds and breast milk components, respectively, α-galactosidase activity or the presence of α-galactosidase encoding genes was more prevalent in a phylogentically distinct group of strains harbouring mostly isolates from the infant gut. Alpha-GOS are dietary fibres present in grains and legumes, and are occasionally added to infant formula [30]. Alpha-Gal 1-3 linkages are found in the histo-blood glyco-antigen type B (Galα1-3(Fucα1-2)Gal) covering the O-glycans in gastrointestinal mucin, which is an endogenous carbohydrate source [53,68]. The presence of α-galactosidase thus enlarges the substrate spectrum of *C. avidum* in the intestine.

Even more conserved than α-galactosidase activity, β-glucuronidase activity and the presence of full-length β-glucuronidase-encoding genes was limited to a subpopulation of *C. avidum*. Beta-glucuronidase activity has been identified in main gut colonizers of the phyla Firmicutes (for e.g. *Faecalibacterium prausnitzii*, *Roseburia* spp.), Bacteroidetes (*Bacteroides fragilis* and *Bacteroides vulgatus*), Actinobacteria (*Bifidobacterium pseudolongum*), and Proteobacteria (*Escherichia coli*), and has been suggested as an adaptive mechanism for metabolism of conjugated dietary compounds (e.g. flavonoids present in breast milk) and endogenous (e.g. bilirubin and steroid hormones) and xenobiotic compounds [12,38,42,48,52]. Glucuronic acid is a component of mucin, and β-glucuronidase activity has been related to mucin utilization in bifidobacteria and to *E. coli* colonization of the intestinal mucus layer [10,47,57]. For strains UCD-PD2, DPC 6544, TM16 and 44067, T14 and MJR7694, genes encoding β-glucuronidase were located in close proximity to genes encoding α-glucosidases and enzymes involved in glucuronate utilization, which could feed into the ED pathway [47]. In agreement, infant isolates of *C. avidum* with β-glucuronidase activity, were able to metabolize glucuronic acid, forming propionate and acetate in a ratio of 1:1, as predicted by the ED pathway [47] and after which pyruvate is oxidized to acetate, and glyceraldehyde-3-phosphate forms propionate via the Wood-Werkman cycle [51].

Virulence traits are less prevalent in a subpopulation of infant fecal isolates

Hemolytic activity on erythrocytes from different species has been previously reported for *C. avidum* strains, and has been associated with a thiol-activated (oxygen-labile) protein of 32 kDa [21,16]. Hemolysis in *C. acnes* isolates from periprosthetic shoulder infections did not seem related to increased pathogenicity [34]; data linking hemolysis to *C. avidum* virulence is lacking. We confirmed hemolytic activity of the type strain ATCC 25577. Hemolysis was previously reported for strain CI882 and we identified additional hemolysis-positive infant fecal and breast milk isolates [1]. The lack of hemolytic activity in infant fecal isolates from the subpopulation could have resulted from gene deletions or mutations, resulting in loss of a function that is not providing ecological benefit in a specific niche [43].

C. avidum *can employ diverse strategies to feed on carbon sources present in the infant gut*

To thrive in the infant gut, *C. avidum* must be able to consume diet- or host-derived substrates or fermentation intermediates provided by other commensals. The ability to consume the fermentation intermediate lactate and glycerol might confer *C. avidum* with a competitive advantage in the infant gut. Lactate is a key metabolite in the infant gut, produced by several infant gut colonizers [5,27,33,49]. Glycerol utilization has been identified as a core function of the early gut microbiome but has not been well investigated [73]. Considering that breast milk has a high content of fat (24–59 g L^{-1}), of which >98% are triacylglycerols (TAG) [15], and that fat absorption is usually incomplete (23–59%), a sizeable concentration of glycerol might be available for microbial utilization in the infant colon [2,37,70]. Additionally, all *C. avidum* infant isolates presented mild activity for the tested lipolytic enzymes (Table S8 in Supplementary material) and consequently might have limited capacity to degrade TAG.

In co-cultures, C. avidum *feeds on lactate and monosaccharides*

Bifidobacterium spp. are dominant colonizers in infants and primary degraders of milk oligosaccharides [18]. Establishment of microbial interactions between *Bifidobacterium* spp. and *C. avidum* in the infant gut depends on the type of complex carbohydrates available and production of lactate. We therefore compared cross-feeding with *B. infantis* and *B. bifidum,* which degrade HMOs with the use of internal and external glycosyl-hydrolases, respectively.

Differences in HMO utilization strategies affected metabolic exchange and SCFA production in co-cultures with *C. avidum* P279. The translocation of intact oligosaccharides followed by intracellular metabolism by *B. infantis* led to mainly lactate cross-feeding with *C. avidum*. Considering the theoretical yield for lactate via the Wood-Werkman cycle, the additional 11.8 mM of propionate formed by *B. infantis*/*C. avidum* co-culture compared to single culture could have originated from the 17.7 mM lactate produced by *B.*

infantis. These results support *in vivo* data in which infant colonization by *Cutibacterium* correlated negatively with fecal lactate at 2 weeks and positively with *Bifidobacterium* abundance at 8 weeks of age [55]. On the other hand, secretion of glycosyl hydrolases and extracellular degradation of HMOs and β-GOS by *B. bifidum* produces di- and monosaccharides for feeding infant isolates of *C. avidum,* explaining the enhanced propionate and acetate formation and disaccharide accumulation during *B. bifidum*/*C. avidum* co-cultures.

The type of carbohydrate influenced cross-feeding between bifidobacteria and *Cutibacterium*. Co-cultures of *C. avidum* P279 with *B. infantis* or *B. bifidum* in mYCFA_L-β-GOS resulted in production of propionate and acetate in a ratio of 2:1, while higher proportions of acetate were detected in co-cultures in mYCFA_HMO. These results indicate that interactions between *Cutibacterium* and bifidobacteria might differ depending on the feeding type of the infant; for example, breast feeding versus feeding infant formula.

Unexpectedly, the growth of the tested bifidobacteria was greatly reduced during co-cultures with *C. avidum* P279, although inoculum concentrations were similar and bifidobacteria had faster kinetics than *C. avidum* single cultures. The reason for this growth reduction is not known, and may not be explained by substrate limitation or product inhibition during initial growth.

Conclusion

Using a novel MLSA screening using five housekeeping genes (*glyS*, *infB*, *rplB*, *pyrG* and *groEL)* in combination with physiologically-based assays, this study was able to reveal genetic and functional heterogeneity of *C. avidum* and suggested the existence of a possible subpopulation of *C. avidum* adapted to the infant gut. Representatives of this subgroup possessed enzymatic activities beneficial in the infant gut and lacked hemolytic activity, which would not contribute to an ecological advantage. The colonization ability of *C. avidum* in the infant gut may relate to ecological adaptation. Our results suggest that *C. avidum* contributes to propionate formation in the infant gut via metabolic cross-feeding with primary degraders such as *Bifidobacterium* spp. Taken together, this study points to *C. avidum* as early infant gut colonizer, in contrast with previous reports focusing on the pathogenic potential of this species.

Funding

This work was supported by own resources (ETH-Zurich and University Children's Hospital Zurich). No additional external funding was received for this study.

Acknowledgements

We thank Alfonso Die, Madeleine Parish and Philipp Rogalla von Bieberstein for their technical assistance and Glycom A/S for supplying HMOs.

Appendix A. Supplementary data

Supplementary material related to this article can be found, in the online version, at doi:https://doi.org/10.1016/j.syapm.2019.05.001.

References

[1] Achermann, Y., Liu, J., Zbinden, R., Zingg, P.O., Anagnostopoulos, A., Barnard, E., Sutter, R., Li, H., McDowell, A., Zinkernagel, A.S. (2018) *Propionibacterium avidum*: a virulent pathogen causing hip periprosthetic joint infection. Clin. Infect. Dis. 66, 54–63, http://dx.doi.org/10.1093/cid/cix665.

[2] Agans, R., Gordon, A., Kramer, D.L., Perez-Burillo, S., Rufián-Henares, J.A., Paliy, O. (2018) Dietary fatty acids sustain growth of human gut microbiota. Appl. Environ. Microbiol. 84, 1–15, http://dx.doi.org/10.1128/AEM.01525-18.

[3] Akkerman, R., Faas, M.M., de Vos, P. (2018) Non-digestible carbohydrates in infant formula as substitution for human milk oligosaccharide functions: effects on microbiota and gut maturation. Crit. Rev. Food Sci. Nutr., http://dx.doi.org/10.1080/10408398.2017.1414030.

[4] Aziz, R.K., Bartels, D., Best, A., DeJongh, M., Disz, T., Edwards, R.A., Formsma, K., Gerdes, S., Glass, E.M., Kubal, M., Meyer, F., Olsen, G.J., Olson, R., Osterman, A.L., Overbeek, R.A., McNeil, L.K., Paarmann, D., Paczian, T., Parrello, B., Pusch, G.D., Reich, C., Stevens, R., Vassieva, O., Vonstein, V., Wilke, A., Zagnitko, O. (2008) The RAST Server: rapid annotations using subsystems technology. BMC Genomics 9, 1–15, http://dx.doi.org/10.1186/1471-2164-9-75.

[5] Backhed, F., Roswall, J., Peng, Y., Feng, Q., Jia, H., Kovatcheva-Datchary, P., Li, Y., Xia, Y., Xie, H., Zhong, H., Khan, M.T., Zhang, J., Li, J., Xiao, L., Al-Aama, J., Zhang, D., Lee, Y.S., Kotowska, D., Colding, C., Tremaroli, V., Yin, Y., Bergman, S., Xu, X., Madsen, L., Kristiansen, K., Dahlgren, J., Wang, J. (2015) Dynamics and stabilization of the human gut microbiome during the first year of life. Cell Host Microbe 17, 690–703, http://dx.doi.org/10.1016/j.chom.2015.04.004.

[6] Belenguer, A., Duncan, S.H., Calder, A.G., Holtrop, G., Louis, P., Lobley, G.E., Flint, H.J. (2006) Two routes of metabolic cross-feeding between *Bifidobacterium adolescentis* and butyrate-producing anaerobes from the human gut. Appl. Environ. Microbiol. 72, 3593–3599, http://dx.doi.org/10.1128/AEM.72.5.3593.

[7] Braegger, C., Chmielewska, A., Decsi, T., Kolacek, S., Mihatsch, W., Moreno, L., Pieścik, M., Puntis, J., Shamir, R., Szajewska, H., Turck, D., van Goudoever, J. (2011) Supplementation of infant formula with probiotics and/or prebiotics: a systematic review and comment by the ESPGHAN committee on nutrition. J. Pediatr. Gastroenterol. Nutr. 52, 238–250, http://dx.doi.org/10.1097/MPG.0b013e3181fb9e80.

[8] Bunesova, V., Lacroix, C., Schwab, C. (2016) Fucosyllactose and L-fucose utilization of infant *Bifidobacterium longum* and *Bifidobacterium kashiwanohense*. BMC Microbiol. 16, 248, http://dx.doi.org/10.1186/s12866-016-0867-4.

[9] Bunesova, V., Lacroix, C., Schwab, C. (2017) Mucin cross-feeding of infant Bifidobacteria and *Eubacterium hallii*. Microb. Ecol. 75, 228–238, http://dx.doi.org/10.1007/s00248-017-1037-4.

[10] Chang, D., Smalley, D.J., Tucker, D.L., Leatham, M.P., Norris, W.E., Stevenson, S.J., Anderson, A.B., Grissom, J.E., Laux, D.C., Cohen, P.S., Conway, T. (2004) Carbon nutrition of *Escherichia coli* in the mouse intestine. Proc. Natl. Acad. Sci. U. S. A. 101, 7427–7432, http://dx.doi.org/10.1073/pnas.0307888101.

[11] Corvec, S. (2018) Clinical and biological features of *Cutibacterium* (formerly *Propionibacterium*) *avidum*, an underrecognized microorganism. Clin. Microbiol. Rev. 31, e00064–17, http://dx.doi.org/10.1128/CMR.00064-17.

[12] Dabek, M., McCrae, S.I., Stevens, V.J., Duncan, S.H., Louis, P. (2008) Distribution of β-glucosidase and β-glucuronidase activity and of β-glucuronidase gene *gus* in human colonic bacteria. FEMS Microbiol. Ecol. 66, 487–495, http://dx.doi.org/10.1111/j.1574-6941.2008.00520.x.

[13] Dahms, P.A., Martin, A.L., Ganz, H.H., Eisen, J.A., Coil, D.A. (2017) Draft genome sequence of *Propionibacterium avidum* strain UCD-PD2 isolated from a feline anal sac. Genome Announc. 5, e00034-17, http://dx.doi.org/10.1128/genomeA.00034-17.

[15] EFSA NDA Panel (Panel on Dietetic Products Nutrition and Allergies), (2014) Scientific opinion on the essential composition of infant and follow-on formulae. EFSA J. 12, 3760, http://dx.doi.org/10.2903/j.efsa.2014.3760.

[16] Fujimura, S., Ko, H.L., Pulverer, G., Jeljaszewicz, J. (1982) Hemolysin of *Propionibacterium avidum*. Zentralbl. Bakteriol. Mikrobiol. Hyg. A 252, 108–115, http://dx.doi.org/10.1016/S0174-3031(82)80094-2.

[17] Garrido, D., Ruiz-Moyano, S., Lemay, D.G., Sela, D.A., German, J.B., Mills, D.A. (2015) Comparative transcriptomics reveals key differences in the response to milk oligosaccharides of infant gut-associated bifidobacteria. Sci. Rep. 5, 13517, http://dx.doi.org/10.1038/srep13517.

[18] Garrido, D., Ruiz-moyano, S., Mills, D.A. (2012) Anaerobe release and utilization of N-acetyl-D-glucosamine from human milk oligosaccharides by *Bifidobacterium longum* subsp. *infantis*. Anaerobe 18, 430–435, http://dx.doi.org/10.1016/j.anaerobe.2012.04.012.

[19] Goh, S.H., Facklam, R.R., Chang, M., Hill, J.E., Tyrrell, G.J., Burns, E.C.M., Chan, D., He, C., Rahim, T., Shaw, C., Hemmingsen, S.M. (2000) Identification of *Enterococcus* species and phenotypically similar *Lactococcus* and *Vagococcus* species by reverse checkerboard hybridization to chaperonin 60 gene sequences. J. Clin. Microbiol. 38, 3953–3959.

[20] González-Rodríguez, I., Gaspar, P., Sánchez, B., Gueimonde, M., Margolles, A., Neves, A.R. (2013) Catabolism of glucose and lactose in *Bifidobacterium animalis* subsp. *lactis*, studied by ^{13}C Nuclear Magnetic Resonance. Appl. Environ. Microbiol. 79, 7628–7638, http://dx.doi.org/10.1128/AEM.02529-13.

[21] Hoeffler, U. (1977) Enzymatic and hemolytic properties of *Propionibacterium acnes* and related bacteria. J. Clin. Microbiol. 6, 555–558.

[22] Human Microbiome Project Consortium, (2012) Structure, function and diversity of the healthy human microbiome. Nature 486, 207–214, http://dx.doi.org/10.1038/nature11234.

[23] Jian, W., Zhu, L., Dong, X. (2001) New approach to phylogenetic analysis of the genus *Bifidobacterium* based on partial HSP60 gene sequences. Int. J. Syst. Evol. Microbiol. 51, 1633–1638, http://dx.doi.org/10.1099/00207713-51-5-1633.

[24] Jost, T., Lacroix, C., Braegger, C.P., Rochat, F., Chassard, C. (2014) Vertical mother-neonate transfer of maternal gut bacteria via breastfeeding. Environ. Microbiol. 16, 2891–2904, http://dx.doi.org/10.1111/1462-2920.12238.

[25] Killer, J., Mekadim, C., Pechar, R., Bunešová, V., Mrázek, J., Vlková, E. (2018) Gene encoding the CTP synthetase as an appropriate molecular tool for identification

and phylogenetic study of the family *Bifidobacteriaceae*. MicrobiologyOpen 7, e00579, http://dx.doi.org/10.1002/mbo3.579.
[26] Killer, J., Skrivanova, E., Hochel, I., Marounek, M. (2015) Multilocus Sequence Typing of *Cronobacter* strains isolated from retail foods and environmental samples. Foodborne Pathog. Dis. 12, 514–521, http://dx.doi.org/10.1089/fpd.2014.1884.
[27] Koenig, J.E., Spor, A., Scalfone, N., Fricker, A.D., Stombaugh, J., Knight, R., Angenent, L.T., Ley, R.E. (2011) Succession of microbial consortia in the developing infant gut microbiome. Proc. Natl. Acad. Sci. U. S. A. 108 (Suppl. 1), 4578–4585, http://dx.doi.org/10.1073/pnas.1000081107.
[29] Kozak, K., Charbonneau, D., Sanozky-dawes, R., Klaenhammer, T. (2015) Characterization of bacterial isolates from the microbiota of mothers' breast milk and their infants. Gut Microbes 6, 341–351, http://dx.doi.org/10.1080/19490976.2015.1103425.
[30] Kruger, C., Zhou, Y., Thorsrud, B.A., Morel-Despeisse, F., Chappuis, E. (2017) Safety evaluation of α-galacto-oligosaccharides for use in infant formulas investigated in neonatal piglets. Toxicol. Res. Appl. 1, 1–10, http://dx.doi.org/10.1177/2397847317722828.
[31] Lewis, A.L., Deitzler, G.E., Ruiz, M.J., Weimer, C., Park, S., Robinson, L.S., Hallsworth-Pepin, K., Wollam, A., Mitreva, M., Lewis, W.G. (2016) Genome sequences of 11 human vaginal Actinobacteria strains. Genome Announc. 4, e00887-16, http://dx.doi.org/10.1128/genomeA.00887-16.
[33] Macfarlane, G.T., Gibson, G.R. (1997) Carbohydrate fermentation, energy transduction and gas metabolism in the human large intestine. In: Mackie, R.I., White, B.A. (Eds.), Gastrointestinal microbiology, chapman & hall microbiology series, Springer, Boston, MA, http://dx.doi.org/10.1007/978-1-4615-4111-0_9.
[34] Mahylis, J.M., Entezari, V., Karichu, J., Richter, S., Derwin, K.A., Iannotti, J.P., Ricchetti, E.T. (2018) Hemolytic strains of *Propionibacterium acnes* do not demonstrate greater pathogenicity in periprosthetic shoulder infections. J. Shoulder Elbow Surg., http://dx.doi.org/10.1016/j.jse.2017.12.025.
[35] Mak, T.N., Schmid, M., Brzuszkiewicz, E., Zeng, G., Meyer, R., Sfanos, K.S., Brinkmann, V., Meyer, T.F., Brüggemann, H. (2013) Comparative genomics reveals distinct host-interacting traits of three major human-associated propionibacteria. BMC Genomics 14, 640, http://dx.doi.org/10.1186/1471-2164-14-640.
[36] Mak, T.N., Yu, S.H., De Marzo, A.M., Brüggemann, H., Sfanos, K.S. (2013) Multilocus sequence typing (MLST) analysis of *Propionibacterium acnes* isolates from radical prostatectomy specimens. Prostate 73, 770–777, http://dx.doi.org/10.1002/pros.22621.
[37] Manson, W.G., Weaver, L.T. (1997) Fat digestion in the neonate. Arch. Dis. Child Fetal 76, 206–211, http://dx.doi.org/10.1136/fn.76.3.F206.
[38] McBain, A.J., Macfarlane, G.T. (1998) Ecological and physiological studies on large intestinal bacteria in relation to production of hydrolytic and reductive enzymes involved in formation of genotoxic metabolites. J. Med. Microbiol. 47, 407–416, http://dx.doi.org/10.1099/00222615-47-5-407.
[39] McGinley, K.J., Webster, G.F., Leyden, J.J. (1978) Regional variations of cutaneous propionibacteria. Appl. Environ. Microbiol. 35, 62–66.
[40] Mekadim, C., Killer, J., Pechar, R., Mrázek, J. (2018) Variable regions of the *glyS*, *infB* and *rplB* genes usable as novel genetic markers for identification and phylogenetic purposes of genera belonging to the family *Propionibacteriaceae*. Int. J. Syst. Evol. Microbiol. 68, 2697–2705, http://dx.doi.org/10.1099/ijsem.0.002873.
[41] Nagpal, R., Kurak, T., Tsuji, H., Takaha, T., Kurakawa, T., Tsuji, H., Takahashi, T., Kawashima, K., Nagata, S., Nomoto, K., Yamashiro, Y. (2017) Evolution of gut *Bifidobacterium* population in healthy Japanese infants over the first three years of life: a quantitative assessment. Sci. Rep. 7, 10097, http://dx.doi.org/10.1038/s41598-017-10711-5.
[42] Koppel, N., Maini Rekdal, V., Balskus, E.P. 2017 Chemical transformation of xenobiotics by the human gut microbiota 2770, http://dx.doi.org/10.1126/science.aag2770.
[43] Ochman, H., Moran, N.A. (2001) Genes lost and genes found: Evolution of bacterial pathogenesis and symbiosis. Science 292, 1096–1098, http://dx.doi.org/10.1126/science.1058543.
[44] Ördögh, L., Hunyadkürti, J. (2013) Complete genome sequence of *Propionibacterium avidum* strain 44067, isolated from a human skin abscess. Genome Announc 1, e00337-13, http://dx.doi.org/10.1128/genomeA.00337-13.
[45] Patrick, S., McDowell, A. (2012) Family I. *Propionibacteriaceae*. genus I. *Propionibacterium*. In: Goodfellow, M., Kämpfer, P., Busse, H.J. (Eds.), Bergey's manual of systematic bacteriology. Volume five. The actinobacteria, Springer, New York, Dordrecht, pp. 1138–1155.
[46] Patterson, E. 2014 Modulation of the gut microbiota and implications for host health. PhD Thesis, University College Cork.
[47] Peekhaus, N., Conway, T. (1998) What's for Dinner? Entner-Doudoroff metabolism in *Escherichia coli*. J. Bacteriol. 180, 3495–3502.
[48] Pellock, S.J., Redinbo, M.R. (2017) Glucuronides in the gut: sugar-driven symbioses between microbe and host. J. Biol. Chem. 292, 8569–8576, http://dx.doi.org/10.1074/jbc.R116.767434.
[49] Pham, V.T., Lacroix, C., Braegger, C.P., Chassard, C. (2016) Early colonization of functional groups of microbes in the infant gut. Environ. Microbiol. 18, 2246–2258, http://dx.doi.org/10.1111/1462-2920.13316.
[50] Pham, V.T., Lacroix, C., Braegger, C.P., Chassard, C. (2017) Lactate-utilizing community is associated with gut microbiota dysbiosis in colicky infants. Sci. Rep. 7, 11176, http://dx.doi.org/10.1038/s41598-017-11509-1.
[51] Piveteau, P. (1999) Metabolism of lactate and sugars by dairy propionibacteria: a review. Le Lait 79, 23–41, http://dx.doi.org/10.1051/lait:199912.
[52] Pollet, R.M., D'Agostino, E.H., Walton, W.G., Xu, Y., Little, M.S., Biernat, K.A., Pellock, S.J., Patterson, L.M., Creekmore, B.C., Isenberg, H.N., Bahethi, R.R., Bhatt, A.P., Liu, J., Gharaibeh, R.Z., Redinbo, M.R. (2017) An atlas of β-Glucuronidases in the human intestinal microbiome. Structure 25, 967–977, http://dx.doi.org/10.1016/j.str.2017.05.003.
[53] Ravcheev, D.A., Thiele, I. (2017) Comparative genomic analysis of the human gut microbiome reveals a broad distribution of metabolic pathways for the degradation of host-synthetized mucin glycans and utilization of mucin-derived monosaccharides. Front. Genet. 8, 111, http://dx.doi.org/10.3389/fgene.2017.00111.
[54] Rinttilä, T., Kassinen, A., Malinen, E., Krogius, L., Palva, A. (2004) Development of an extensive set of 16S rDNA-targeted primers for quantification of pathogenic and indigenous bacteria in faecal samples by real-time PCR. J Appl Microbiol. 97, 1166–1177, http://dx.doi.org/10.1111/j.1365-2672.2004.02409.x.
[55] Rocha Martin, V.N., Schwab, C., Krych, L., Voney, E., Geirnaert, A., Braegger, C., Lacroix, C. (2019) Colonization of *Cutibacterium avidum* during infant gut microbiota establishment. FEMS Microbiol. Ecol. 95, fiy215, http://dx.doi.org/10.1093/femsec/fiy215.
[56] Rodriguez-R, L.M., Konstantinidis, K.T. (2016) The enveomics collection: a toolbox for specialized analyses of microbial genomes and metagenomes. Peer J. Preprints 4, e1900v1, http://dx.doi.org/10.7287/peerj.preprints.1900v1.
[57] Ruiz, L., Gueimonde, M., Couté, Y., Salminen, S., Sanchez, J.C., De Los Reyes-Gavilán, C.G., Margolles, A. (2011) Evaluation of the ability of *Bifidobacterium longum* to metabolize human intestinal mucus. FEMS Microbiol. Lett. 314, 125–130, http://dx.doi.org/10.1111/j.1574-6968.2010.02159.x.
[58] Scholz, C.F.P., Kilian, M. (2016) The natural history of cutaneous propionibacteria and reclassification of selected species within the genus *Propionibacterium* to the proposed novel genera *Acidipropionibacterium* gen. nov., *Cutibacterium* gen. nov. and *Pseudopropionibacterium* gen. nov. Int. J. Syst. Evol. Microbiol. 66, 4422–4432, http://dx.doi.org/10.1099/ijsem.0.001367.
[59] Sela, D.A., Chapman, J., Adeuya, A., Kim, J.H., Chen, F., Whitehead, T.R., Lapidus, A., Rokhsar, D.S., Lebrilla, C.B., German, J.B., Price, N.P., Richardson, P.M., Mills, D.A. (2008) The genome sequence of *Bifidobacterium longum* subsp. *infantis* reveals adaptations for milk utilization within the infant microbiome. Proc. Natl. Acad. Sci. U. S. A. 105, 18964–18969, http://dx.doi.org/10.1073/pnas.0809584105.
[62] Stewart, C.J., et al. (2018) Temporal development of the gut microbiome in early childhood from the TEDDY study. Nature 562, 583–588, http://dx.doi.org/10.1038/s41586-018-0617-x.
[63] Stoddard, S.F., Smith, B.J., Hein, R., Roller, B.R.K., Schmidt, T.M. (2015) rrnDB: improved tools for interpreting rRNA gene abundance in bacteria and archaea and a new foundation for future development. Nucleic Acids Res. 43, 593–598, http://dx.doi.org/10.1093/nar/gku1201.
[64] Tamura, K., Stecher, G., Peterson, D., Filipski, A., Kumar, S. (2013) MEGA6: molecular evolutionary genetics analysis version 6.0. Mol. Biol. Evol. 30, 2725–2729, http://dx.doi.org/10.1093/molbev/mst197.
[65] Torres, D.P.M., do P.F. Gonçalves, M., Teixeira, J.A., Rodrigues, L.R. (2010) Galacto-Oligosaccharides: production, properties, applications, and significance as prebiotics. Compr. Rev. Food Sci. Food Saf. 9, 438–454, http://dx.doi.org/10.1111/j.1541-4337.2010.00119.x.
[66] Urbaniak, C., Cummins, J., Brackstone, M., Macklaim, J.M., Gloor, G.B., Baban, C.K., Scott, L., O'Hanlon, D.M., Burton, J.P., Francis, K.P., Tangney, M., Reid, G. (2014) Microbiota of human breast tissue. Appl. Environ. Microbiol. 80, 3007–3014, http://dx.doi.org/10.1128/AEM.00242-14.
[67] Vazquez-Gutierrez, P., Lacroix, C., Jaeggi, T., Zeder, C., Zimmerman, M.B., Chassard, C. (2015) Bifidobacteria strains isolated from stools of iron deficient infants can efficiently sequester iron. BMC Microbiol. 15, 3, http://dx.doi.org/10.1186/s12866-014-0334-z.
[68] Wakinaka, T., Kiyohara, M., Kurihara, S., Hirata, A., Chaiwangsri, T., Ohnuma, T., Fukamizo, T., Katayama, T., Ashida, H., Yamamoto, K. (2013) Bifidobacterial α-galactosidase with unique carbohydrate-binding module specifically acts on blood group B antigen. Glycobiology 23, 232–240, http://dx.doi.org/10.1093/glycob/cws142.
[69] Wang, Z., Yang, S.T. (2013) Propionic acid production in glycerol/glucose co-fermentation by *Propionibacterium freudenreichii* subsp. *shermanii*. Bioresour. Technol. 137, 116–123, http://dx.doi.org/10.1016/j.biortech.2013.03.012.
[70] De Weirdt, R., Possemiers, S., Vermeulen, G., Moerdijk-Poortvliet, T.C.W., Boschker, H.T.S., Verstraete, W., Van De Wiele, T. (2010) Human faecal microbiota display variable patterns of glycerol metabolism. FEMS Microbiol. Ecol. 74, 601–611, http://dx.doi.org/10.1111/j.1574-6941.2010.00974.x.
[71] Wildeman, P., Brüggemann, H., Scholz, C.F.P., Leimbach, A., Söderquist, B. (2016) *Propionibacterium avidum* as an etiological agent of prosthetic hip joint infection. PLoS One 11, e0158164, http://dx.doi.org/10.1371/journal.pone.0158164.
[72] Wood, H.G. (1981) Metabolic cycles in the fermentation by propionic acid bacteria. Curr. Top. Cell. Regul. 18, 255–287.
[73] Xiong, W., Brown, C.T., Morowitz, M.J., Banfield, J.F., Hettich, R.L. (2017) Genome-resolved metaproteomic characterization of preterm infant gut microbiota development reveals species-specific metabolic shifts and variabilities during early life. Microbiome 5, 72, http://dx.doi.org/10.1186/s40168-017-0290-6.
[74] Yin, Y., Mao, X., Yan, J., Chen, X., Mao, F., Xu, Y. (2012) DbCAN: a web resource for automated carbohydrate-active enzyme annotation. Nucleic Acids Res. 40, W445–W451, http://dx.doi.org/10.1093/nar/gks479.